Gapping by Squashing: Metal-Insulator and Insulator-Metal Transitions in Collapsed Carbon Nanotubes

Paul E. Lammert, Peihong Zhang, and Vincent H. Crespi

Department of Physics and Center for Materials Physics, The Pennsylvania State University, 104 Davey Lab, University Park, Pennsylvania 16802

(Received 29 April 1999)

Squashing brings circumferentially separated areas of a carbon nanotube into close proximity, drastically altering the low-energy electronic properties and (in some cases) reversing standard rules for metallic versus semiconducting behavior. Such a deformation mode, not requiring motion of tube ends, may be useful for devices. Uniaxial stress of a few kbar can reversibly collapse a small-radius tube, inducing a 0.1 eV gap with a very strong pressure dependence, while the collapsed state of a larger tube is stable. The low-energy electronic properties of chiral tubes are surprisingly insensitive to collapse.

PACS numbers: 71.20.Tx, 77.65.–j, 85.40.Ux

Combined with the nontrivial nanometer-scale morphology of carbon nanotubes [1], the unique Fermi level structure of graphene opens several routes for manipulating the low-energy electronic properties of nanotubes through structural deformations. Unfortunately, the structural perturbations considered to date, such as twisting [2], bending [3], stretching [4], and topological defects [5], require either motion of the tube ends, which is not compatible with stable contacts for devices, or changes to the sp^2 bonding framework, which is a difficult and irreversible modification. Here we describe the important electronic consequences of a new, low-energy deformation—transverse collapse—which can be imposed locally with relative ease without disturbing the bond topology or the positions of the tube ends. A perturbative treatment with a clear interpretation reveals three general classes of response: gap induction, metallization, or a surprising electronic insensitivity to collapse. In some cases, collapse actually reverses the standard rules for semiconducting versus metallic behavior. The perturbative picture is fully supported by four-orbital tight binding and density functional calculations.

Nanotubes are prone to significant cross-sectional deformation, as evidenced by observations of complete collapse [6] (see Fig. 1) and the gentler influence of substrates and electrical contacts on tube cross section [8]. Large-radius thin-walled tubes are most susceptible, but smaller-radius and multiwalled tubes can also collapse. Above roughly 12 Å radius the flattened state is stable or metastable; below this size an external force can induce a reversible collapse. This crossover lies within the range (0.7–3 nm) over which the radii of single-walled tubes can currently be varied by changes in synthesis temperature [9], introduction of sulfur [10], and fusion of tubes [11].

A cylindrical carbon nanotube [1] is metallic or semiconducting depending upon its wrapping indices (i.e., the circumference expressed in graphene lattice coordinates) [12]. Here we analyze the electronic consequences of a complete transverse collapse wherein opposing internal faces of the tube come into contact. This new interlayer coupling dominates the low-energy electronic properties over an energy range of 0.1–0.2 eV. In particular, metallic (n, n) tubes become semiconductors and narrow-gap $(3n, 0)$ tubes can be metallized. The electronic properties of most other tubes are essentially unchanged by this deformation. The first two classes allow local tuning of electronic properties, while the third may have special application in situations which require stable functionality (e.g., electrical interconnects). In certain tubes the sensitivity of band gap to uniaxial pressure is very high, more than an order of magnitude larger than observed in silicon and diamond [13]. These distinct behaviors under tube collapse may carry significant implications for producing robust and/or tunable nanoscale electronic devices.

Tube collapse changes the electronic structure through two mechanisms: the creation of inhomogenous curvature and the new coupling introduced between interior faces. We focus on the new coupling across the medial bilayer. Later we discuss the additional curvature effects, which do not affect the essential results. We begin by analyzing an infinite graphene bilayer. The first Brillouin zone of a graphene sheet has Fermi points at K and K' [14] (see Fig. 2). Each Fermi point contains two degenerate states; we choose them to be nonzero on only the A or B sublattice, respectively. Under a real-space translation incrementing $x_{\pm}$ by one (see Fig. 3), the states at K acquire phases $e^{\pm i2\pi/3}$. Figure 3 shows the strength of the coupling V_{bi} between the A-sublattice states on the two sheets,

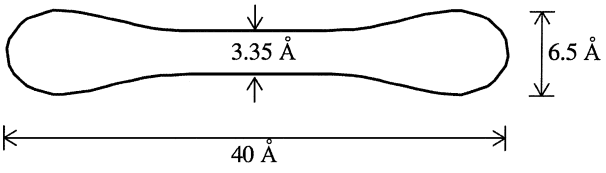

FIG. 1. Cross section of a collapsed $(20, 20)$ tube under zero external force as determined by tight-binding total-energy techniques, including the interlayer attraction [7]. We call the central region a quasibilayer.

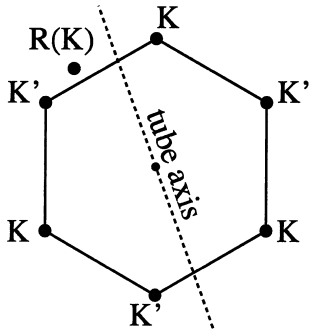

FIG. 2. The quasibilayer coupling mixes states with **k**'s related by reflection across the tube axis. For generic wrapping angles χ, the reflection of K (or K') misses another such point by $2|K|\sin\tilde{\chi}$, where $\tilde{\chi}$ is the absolute value of the difference of χ from the nearest multiple of $\pi/6$.

as a function of their relative horizontal offset. The coupling is maximum at A/A stacking and vanishes for A/B stacking. In Fourier expansion,

$$V_{\rm bi}^{\rm AA} \approx \frac{V_0(c)}{3}\, e^{(2i\pi/3)(x_+ - x_-)}[1 + e^{2\pi i x_-} + e^{-2\pi i x_+}] \tag{1}$$

has only one free parameter: the strength $V_0(c)$ depending on sheet separation c [15]. The higher-order Fourier components are at least 100 times smaller than these first three, even at $c = 3$ Å. To within better than 5% accuracy, $V_0(c) = \exp[2.8(2.68 - c/\text{Å})]$ eV for 3.0 Å $\leq c \leq$ 3.5 Å. The couplings between the other three pairs of sublattices are obtained by obvious modifications.

In the infinite bilayer, states at K in the two sheets are coupled since their relative phase is uniform. However, in a nanotube the states at K couple most strongly to states at $R(K)$, *the reflection of K across the axis of the tube* (see Fig. 2). The operation $R(\cdot)$ can be illustrated by drawing arrows around the circumference of a transparent cylinder to represent the graphitic **k**, then collapsing the tube. This construction indicates three classes of narrow-gap tubes. The low-energy electronic structure of large-gap semiconducting tubes is only slightly perturbed by collapse, so we do not consider them at all. For an (n, n) tube (wrapping angle $\chi = 0$) [16], K couples to itself, yielding a pair of identical two-band problems at K and K'. In a $(3n, 0)$ tube ($\chi = \pi/6$), K couples to K', thereby producing a four-band problem. For a generic narrow-gap $(n + 3m, n)$ tube, the reflection of K across the axis lies far from a Fermi point; this large energy mismatch greatly weakens the effects of the coupling. We now discuss each case using both four-orbital nonorthogonal tight-binding [17] and perturbation theory.

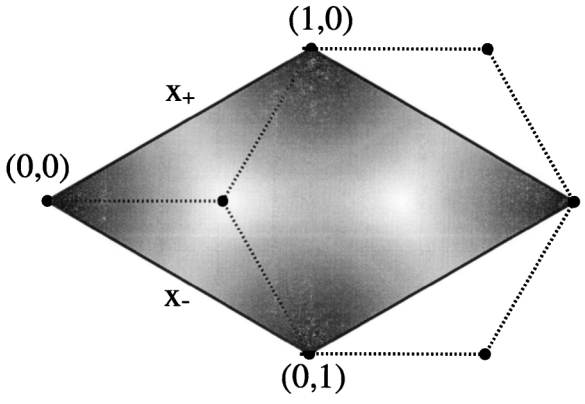

FIG. 3. Grey scale plot of strength $|V_{\rm bi}^{AA}|^2$ of the bilayer coupling. The coordinate x_+ (x_-) runs from 0 to 1 going northeast (southeast), giving the shift of the lower lattice relative to the top one (shown). Dark (light) regions near A/A (A/B) stacking indicate strong (weak) coupling (zero at A/B).

A cylindrical (n, n) nanotube has no gap, and the inhomogeneity of curvature and bond strain under squashing will not alter that. Any gapping arises purely from quasibilayer coupling, which gives this case special interest. Two nearly conical bands evolve from the A- and B-sublattice states at K (the situation at K' is identical and independent). Averaged over the regions of the tube which are in close proximity, the bilayer Hamiltonian [Eq. (1)] describes their coupling. A "tank-treading" motion of the atoms along the circumference will alter the quasibilayer registry, but for an (n, n) tube the variation is restricted to $x_+ = x_- \equiv x$ (see Fig. 3). The coupling results in a quadratic dispersion,

$$(\varepsilon - \varepsilon_0)^2 = \left(\frac{\Delta_0}{2}\right)^2 + v_{\rm F}^2(q - q_0)^2, \tag{2}$$

centered around the point $q_0 = \overline{V}_0(1 + 2\cos 2\pi x)/3v_{\rm F}$ and exhibiting a gap $\Delta_0 = 2\overline{V}_0|\sin 2\pi x|/\sqrt{3}$. Here, $v_{\rm F}$ is the graphene Fermi velocity, energy and **k** vector are measured from the Fermi point for the tube with quasibilayer coupling turned off, and $\overline{V}_0$ is a coupling averaged over the varying bilayer separation. The rigid shift in energy, $\varepsilon_0 = \overline{V}_0(1 - \cos 2\pi x)/3$, is irrelevant for a uniformly squashed nanotube, but becomes relevant for tubes which also have uncollapsed cylindrical regions along their length. For large tubes, the spacing is essentially constant over the central region, so that $\overline{V}_0$ is approximately V_0 times the fraction of the tube in close contact. Tight binding (Fig. 4) gives $\overline{V}_0 = 40$ meV, producing a gap of 45 meV at $x = 1/4$ for the collapsed $(20, 20)$ tube, rising to 100 meV under 10 kbar uniaxial stress. Under 6 kbar, a smaller-radius $(10, 10)$ nanotube with $x = 1/4$ develops a gap of 25 meV. Upon release of the stress, this nanotube reverts to a cylindrical shape.

To check the accuracy of these results, we performed pseudopotential local density approximation (LDA) calculations on an infinite graphene bilayer at A/A stacking. Over the range of separations of 3–4 Å, the tight-binding and LDA results agree very well up to a constant scale factor, which indicates that our perturbative and tight-binding results for energies and **k** shifts should simply be scaled up by a factor of 1.5 to 2. Taking this correction into

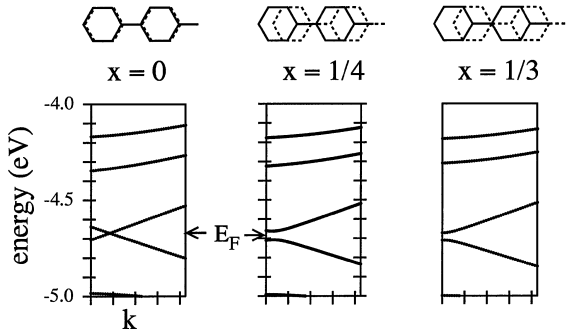

FIG. 4. Closeups of the band structures of the collapsed $(20, 20)$ tube shown in Fig. 1, with the lattice offsets x shown on top. Although $x = 0$ looks like A/A stacking, following the lattice around the bend of the tube reveals it to be A/B. The tight-binding results agree very well with the perturbative results in the text for $\overline{V}_0 = 40$ meV. The **k** tick marks are spaced by 4×10^{-3} atomic units; the entire span shown is $1/85$ of the Brillouin zone.

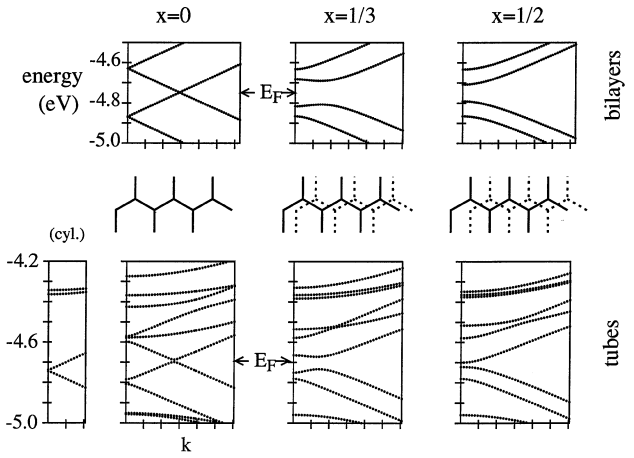

FIG. 5. Tight-binding bands near the Fermi level for a collapsed $(36, 0)$ nanotube (bottom), and corresponding slices through the zone of a graphene bilayer (top). At $x = 0$ the bonding/antibonding split of $4\overline{V}_0$ produces a gapless situation, while for x much different, the bilayer coupling creates a band gap (or significantly enlarges it for a nanotube). The scale of **k** is as in Fig. 4, spanning $1/30$ of the Brillouin zone in total.

account, the collapse of (n, n) tubes induces band gaps from 0–4 times room temperature at zero pressure and up to $\sim$10 times kT_{room} at moderate ($\sim$ kbar) pressures. These gaps could be imposed through modest external forces in relatively localized regions without disturbing the remainder of the tube. Previously considered deformations (e.g., stretching, bending, or twisting) typically require much higher energies to create and also require that tube ends be moved, a requirement incompatible with most device applications.

In contrast to (n, n) tubes, those of index $(3n, 0)$ have small curvature-induced gaps which scale as R^{-2}. A $(36, 0)$ nanotube having roughly the same radius as a $(20, 20)$ tube exhibits an 8 meV gap, which is much smaller than the perturbations induced by collapse. Under collapse, states at K are coupled to those at K', and the allowed interlayer registries are $x_- = 0$ with $x \equiv x_+$ arbitrary, or vice versa. For $x = 0$, bilayer eigenstates are easily seen to be bonding and antibonding combinations of states on the two sheets. As shown in the first plot of Fig. 5, this creates a pair of cones, one shifted up, one down, from the single-sheet position. The cones cross at the Fermi level, so the nanotube is gapless and remains gapless even when curvature destroys the degeneracies at the apices. In this special case, the collapse of a $(3n, 0)$ nanotube can actually *remove* the curvature-induced band gap and restore metallic behavior. *Tube collapse causes metallic (n, n) tubes to become semiconducting and can also cause small-gap semiconducting tubes to become metallic.* This is a reversal of the standard wrapping-index rules for tube electronic structure [12].

For $x \neq 0$ in $(3n, 0)$ tubes, the quasibilayer coupling creates a band gap which is typically much larger than the curvature-induced gap of the nanotube. Figure 5 shows the close relationship between the $(36, 0)$ nanotube electronic states (within four-orbital nonorthogonal tight binding) and the appropriate slices through the infinite bilayer band structure. The scale of the low-energy perturbations $\overline{V}_0$ is consistent with the results for the $(20, 20)$ tube. For a general registry, the Fermi level degeneracy is destroyed by the bilayer coupling with no overall shift of the bands. The small shift evident in Fig. 5 arises from inhomogeneous curvature (see below).

For all wrapping indices not in the first two categories, states near the Fermi level are coupled to states far from it (see Fig. 2). K couples to a state approximately $2\tilde{\chi} v_{\text{F}}/a_0$ higher in energy, with a strength of roughly $\overline{V}_0/\sqrt{3}$, the rms average of $V(x_+, x_-)$ over relative interlayer registries. This large energy mismatch means that such tubes are very robust electronically under collapse.

Quasibilayer coupling, acting alone (neglecting curvature), creates a gap estimated [18] as $\Delta_B \approx a_0 \overline{V}_0^2/(3 v_{\text{F}} \tilde{\chi})$ ($a_0 = 2.46$ Å is the graphene lattice constant). For a tube of radius comparable to that of Fig. 5, $\Delta_B \approx 0.25\,\text{meV}/\sin\chi$. By comparison, even the small curvature-induced gap is typically much larger: $\Delta_K \approx 8\,\text{meV}\,\sin 3\chi$. Interlayer coupling could be mediated by emission or absorption of a phonon whose wave vector spans the **k** mismatch between the nearly isoenergetic states, similar to the situation between tubes of differing chirality in a bundle [19]. This type of phonon-assisted hopping contrasts with the more familiar variety in that the phonon is required to supply wave vector rather than energy. This electronic stability under an easily imposed deformation might prove relevant to future applications. In fact, one could argue that it is *too* easy to perturb the low-energy properties of carbon nanotubes, because of the ease with which the Fermi-level degeneracy can be broken. In such a case, the surprising stability of these chiral tubes may have a special value. Note also that a similar wave vector mismatch can occur

between the layers of multiwalled tubes, effectively decoupling adjacent walls.

In addition to the quasibilayer coupling, the inhomogeneous curvature induced by collapse also modifies the electronic states. To good approximation, this merely augments the preexisting curvature-induced perturbations (coupling to curvature is local). For the cross section of Fig. 1, this effect increases the preexisting gap and band shift by twofold or threefold. This effect, included in the tight-binding results presented above, is significantly smaller than the bilayer coupling itself. Furthermore, in the (n, n) tube the inhomogeneous curvature has essentially no effect. Although a perturbative analysis will break down at very large curvatures, the good agreement between perturbation theory and the tight-binding results (which are sensitive to rehybridization) indicates that the cross sections studied here are safely in the perturbative regime for the low-energy properties. This contrasts with the more severe distortions present in the collapsed state associated with sharp localized bends [3].

In conclusion, the electronic response from nanotube collapse reveals two sharply contrasting behaviors. Some tubes—(n, n) and $(3n, 0)$—have an extreme sensitivity to transverse pressure which arises from the delicate nature of the degenerate low-energy electronic states and the softness of nanotubes under transverse deformations. Other tubes exhibit a surprising insensitivity to collapse: wave vector mismatch arising from the low dimensionality and the semimetallic nature of the host material prevents significant coupling, even when previously isolated metallic regions are brought into direct contact. Since these deformations can be reversibly imposed in well-defined regions with a minimal energetic cost and no motion of the tube ends, they might become relevant to future applications in small-scale devices.

We thank E. Hernandez for valuable advice in the development of the tight-binding code and J. Patel for stimulating discussions. We gratefully acknowledge the David and Lucile Packard Foundation, the National Science Foundation through Grant No. DMR-9876232, the Research Corporation, and both the National Partnership for Advanced Computational Infrastructure and the Center for Academic Computing at the Pennsylvania State University for computational support.

[1] S. Iijima, Nature (London) **354**, 56 (1991).
[2] C. L. Kane and E. J. Mele, Phys. Rev. Lett. **78**, 1932 (1997).
[3] A. Rochefort, F. Lesage, D. R. Salahub, and Ph. Avouris, e-print cond-mat/9904083; A. Rochefort, D. R. Salahub, and Ph. Avouris, Chem. Phys. Lett. **297**, 45 (1998).
[4] R. Heyd, A. Charlier, and E. McRae, Phys. Rev. B **55**, 6820 (1997); V. H. Crespi, M. L. Cohen, and A. Rubio, Phys. Rev. Lett. **79**, 2093 (1997); P. Zhang, P. E. Lammert, and V. H. Crespi, Phys. Rev. Lett. **81**, 5346 (1998).
[5] L. Chico, V. H. Crespi, L. X. Benedict, S. G. Louie, and M. L. Cohen, Phys. Rev. Lett. **76**, 971 (1996).
[6] N. G. Chopra, L. X. Benedict, V. H. Crespi, M. L. Cohen, S. G. Louie, and A. Zettl, Nature (London) **377**, 135 (1995); L. X. Benedict, V. H. Crespi, N. G. Chopra, A. Zettl, M. L. Cohen, and S. G. Louie, Chem. Phys. Lett. **286**, 490 (1998).
[7] P. Zhang and V. H. Crespi, Phys. Rev. Lett. **83**, 1791 (1999).
[8] T. Hertel, R. E. Walkup, and Ph. Avouris, Phys. Rev. B **58**, 13 870 (1998).
[9] S. Bandow, S. Asaka, Y. Saito, A. M. Rao, L. Grigorian, E. Richter, and P. C. Eklund, Phys. Rev. Lett. **80**, 3779 (1998).
[10] C.-H. Kiang, W. A. Goddard III, R. Beyers, J. R. Salem, and D. S. Bethune, J. Phys. Chem. **98**, 6612 (1994).
[11] P. Nikolaev, A. Thess, A. G. Rinzler, D. T. Colbert, and R. E. Smalley, Chem. Phys. Lett. **266**, 422 (1997).
[12] R. Saito, M. Fujita, G. Dresselhaus, and M. S. Dresselhaus, Appl. Phys. Lett. **60**, 2204 (1992); N. Hamada, S. Sawada, and A. Oshiyama, Phys. Rev. Lett. **68**, 1579 (1992); J. W. Mintmire, B. I. Dunlap, and C. T. White, Phys. Rev. Lett. **68**, 631 (1992).
[13] P. E. Van Camp, V. E. Van Doren, and J. T. Devreese, Phys. Rev. B **34**, 1314 (1986).
[14] See, for example, D. P. DiVincenzo and E. J. Mele, Phys. Rev. B **29**, 1685 (1984).
[15] Note that $V_0(c)$ is very nearly equal to the tight-binding parameter $H_{pp\sigma}(c)$.
[16] The wrapping angle χ is defined as the angle between the circumferential direction of the nanotube and a bond. One may take χ to lie in the interval $[0, \pi/6)$. Some refer to this as the "chiral angle" or "helical angle."
[17] We use parameters developed by D. Porezag, Th. Frauenheim, Th. Köhler, G. Seifert, and R. Kaschner, Phys. Rev. B **51**, 12 947 (1995).
[18] This is a second order calculation, which is valid if $\tilde{\chi} > \chi_c = a\overline{V}_0/(2\sqrt{3}\,\upsilon_F) \approx \overline{V}_0/(7.6\ \mathrm{eV})$. With $\overline{V}_0$ in the range of a few tens of meV, almost any tube other than $(n, 0)$ or (n, n) satisfies this criterion.
[19] E. J. Mele and C. Kane (private communication).